Band-edge excitons in PbSe nanocrystals and nanorods

J. G. Tischler, T. A. Kennedy, E. R. Glaser, Al. L. Efros, E. E. Foos, J. E. Boercker, T. J. Zega, R. M. Stroud, and S. C. Erwin
Naval Research Laboratory, Washington, DC 20375, USA
(Received 1 October 2010; published 6 December 2010)

We investigate the fine structure of band-edge excitons in PbSe nanocrystals and nanorods using circularly polarized magnetophotoluminescence and optically detected magnetic resonance and, based on the results, propose a singlet-triplet model of exciton photoluminescence from nondegenerate conduction and valence bands. From the data and model we extract g-factors for electrons and holes of +1.2 and +0.8, respectively. The splitting of the triplet ground state, which is responsible for the low-temperature photoluminescence, is 88 μeV for nanorods, and less than 20 μeV for nanocrystals. The intervalley splitting of the electron and hole levels in the nanocrystals is much larger than the electron-hole exchange interaction.

DOI: 10.1103/PhysRevB.82.245303 PACS number(s): 71.35.Ji, 78.67.Bf, 78.67.Qa, 78.66.−w

Advances in the fabrication and understanding of colloidally grown nanocrystal (NC) quantum dots and nanorods (NRs) have been driven by intense interest in their potential applications. These applications include biological labels[1–3] as well as tunable optoelectronic devices such as light emitting diodes,[4] lasers,[3,5] detectors,[6] and photovoltaics.[7–11] NCs of the lead chalcogenides (PbS, PbSe, and PbTe) offer distinct advantages for such applications. Lead chalcogenides are semiconductors with a direct narrow gap that can be tuned by quantum confinement over a range of wavelengths suited to different applications, including ones operating in the infrared transparency windows centered at 1.3 and 1.6 μm, as well as planar optical waveguides,[12] *in vivo* imaging of biological tissue,[13] and photovoltaic conversion.[7–9] The absorption spectra of lead chalcogenide (specifically, PbSe) NCs are well understood from the work by Kang and Wise.[14] But their photoluminescence (PL) properties and the fine structure of the band-edge exciton spectra, which controls these properties, are still controversial.[15–17]

Lead chalcogenides have a direct gap at the L point of the Brillouin zone. The fourfold degeneracy of the L point means that the 1s ground states of both electrons and holes in lead chalcogenide NCs are eightfold degenerate (including spin), and thus there are $8\times 8=64$ transitions between band-edge excitons. In spherical NCs, these electron and hole states split into two sublevels due to the intervalley interaction,[14] as found in first-principles calculations of NC energy spectra.[16] The fine structure of these states is a complicated function of the relative strength of the intervalley interaction, the electron-hole exchange interaction, and deviations of the NC shape from spherical symmetry. The high degree of degeneracy renders fluorescence line-narrowing experiments [which were previously used to study band-edge excitons in CdSe NCs (Refs. 18–20)] inefficient, highlighting the need for a different approach.

In this paper we use circularly polarized magnetophotoluminescence (CP-MPL) and optically detected magnetic resonance (ODMR) (Refs. 21 and 22) to study the fine structure of the band-edge excitons in PbSe NCs and NRs. Our results are well described by the standard singlet-triplet model of the exciton PL from nondegenerate electrons and holes, suggesting that intervalley splitting does not significantly affect the PL. Our results also confirm the much-discussed near-mirror symmetry of electron and hole spectra in PbSe NCs. Finally, we extract numerical values for the electron and hole g factors and the electron-hole exchange interaction.

We studied PbSe NCs having two basic shapes: either spherically symmetric (i.e., NCs) or slightly elongated in one direction (i.e., NRs), with diameters of approximately 4 nm. Samples were purchased from Evident Technologies as well as synthesized in-house using published techniques.[23]

Transmission electron microscopy (TEM) images of two samples are shown in Fig. 1. Sample 1 [Fig. 1(a)] consists of spherical NCs with average diameter 4.5 nm and size dispersion ±5%. The composition of the samples was confirmed by energy-dispersive x-ray spectroscopy (EDS), whereas structure was verified by measuring the lattice constant from high-resolution TEM (HRTEM) images. Sample 2 [Fig. 1(b)]

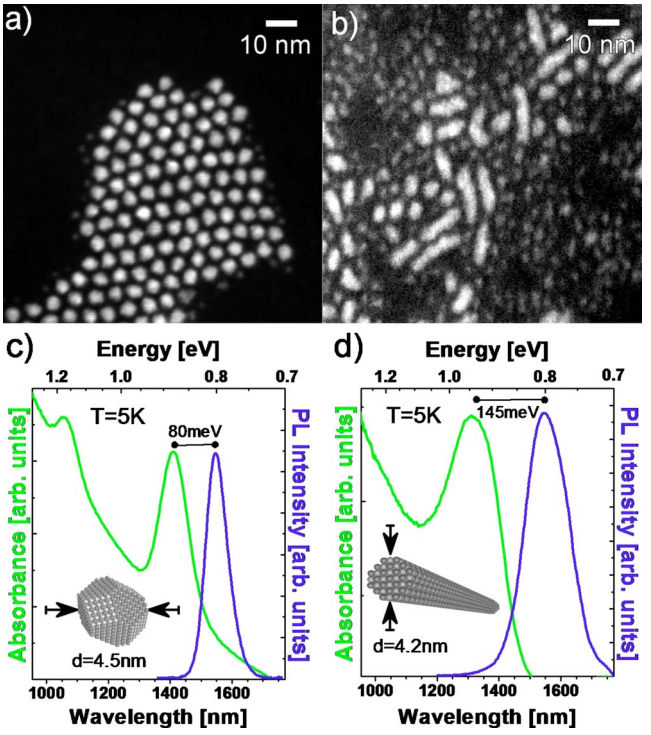

FIG. 1. (Color online) (a) Z-contrast TEM for PbSe NCs and (b) [001]-oriented PbSe NRs. (c) Photoluminescence (blue line) and absorbance (green line) measured in 4.5-nm-diameter PbSe NCs at $T=5$ K and (d) in 4.2-nm-diameter PbSe NRs at $T=5$ K.

Report Documentation Page

Form Approved
OMB No. 0704-0188

1. REPORT DATE	2. REPORT TYPE	3. DATES COVERED
OCT 2010		**00-00-2010 to 00-00-2010**

4. TITLE AND SUBTITLE	5a. CONTRACT NUMBER
Band-edge excitons in PbSe nanocrystals and nanorods	5b. GRANT NUMBER
	5c. PROGRAM ELEMENT NUMBER
6. AUTHOR(S)	5d. PROJECT NUMBER
	5e. TASK NUMBER
	5f. WORK UNIT NUMBER
7. PERFORMING ORGANIZATION NAME(S) AND ADDRESS(ES) **Naval Research Laboratory,Washington,DC,20375**	8. PERFORMING ORGANIZATION REPORT NUMBER
9. SPONSORING/MONITORING AGENCY NAME(S) AND ADDRESS(ES)	10. SPONSOR/MONITOR'S ACRONYM(S)
	11. SPONSOR/MONITOR'S REPORT NUMBER(S)

12. DISTRIBUTION/AVAILABILITY STATEMENT
Approved for public release; distribution unlimited

13. SUPPLEMENTARY NOTES

14. ABSTRACT

15. SUBJECT TERMS

16. SECURITY CLASSIFICATION OF:			17. LIMITATION OF ABSTRACT	18. NUMBER OF PAGES	19a. NAME OF RESPONSIBLE PERSON
a. REPORT	b. ABSTRACT	c. THIS PAGE			
unclassified	**unclassified**	**unclassified**	**Same as Report (SAR)**	**6**	

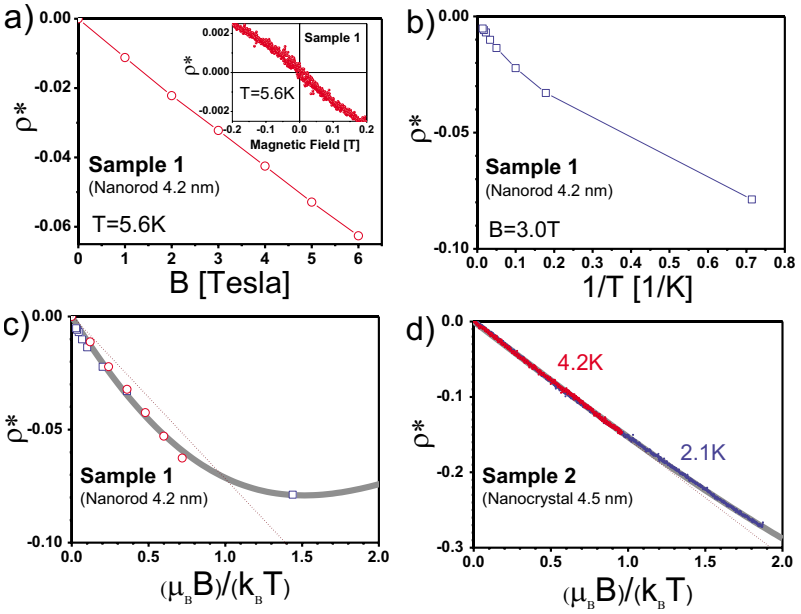

FIG. 2. (Color online) (a) Dependence of the PL polarization of PbSe NRs on magnetic field, (b) on inverse temperature $1/T$, and (c) on the dimensionless variable $(\mu_B B/k_B T)$. (d) Dependence the PL polarization of PbSe NCs on the dimensionless variable $(\mu_B B/k_B T)$.

consists of a mixture of NRs with average diameter 4.2 nm and average length 13 nm, and small spherical NCs with diameter ~3 nm. HRTEM shows that the nanorods were elongated along the [001] direction.

The photoluminescence peak corresponding to the $1s_e$-$1s_h$ transition was at 800 meV (1.55 μm) for both samples, as shown in Figs. 1(c) and 1(d) at 4K. For sample 1 the full width at half maximum (FWHM) was ~80 meV, consistent with the size inhomogeneity determined from HRTEM. For sample 2 the FWHM was significantly larger (~50% larger than for sample 1). Comparison of the PL and absorbance spectra at 4 K shows that the Stokes shift for sample 1 is significantly smaller than for sample 2. Sample 1 shows an absorption transition at 1.05 μm, which has been previously identified as $1s_e$-$1p_h/1s_h$-$1p_e$, while sample 2 does not show this transition. The larger Stokes shift and PL peak FWHM observed in sample 2, and the absence of the $1s_e$-$1p_h/1s_h$-$1p_e$ transition,[24] are consistent with previous results on PbSe semiconductor NRs at room temperature.[25] These features most likely arise from inhomogeneities in the NR radius which lead to localization of excitons in different parts of the NR.[26] Sample 2 also shows a weak PL peak at ~1000 nm (not shown) originating from the 3 nm NCs, as previously reported for NCs of this size.[24]

We were able to study optical properties of NRs using sample 2 although this sample is a mixture of NRs and NCs. This is because the PL spectra of 3-nm-diameter NCs and 4.2-nm-diameter NRs are well resolved spectrally and do not overlap. Furthermore, the transmission and photoluminescence data for sample 2 [Fig. 2(d)] in the NR spectral region are in very good agreement with those results measured in monodisperse homogeneous NRs at room temperature.[25] This shows a quite high homogeneity of NR size and shape in sample 2.

The CP-MPL spectra were obtained by first immersing the samples in a liquid helium-bath cryostat equipped with a split-coil superconducting magnet. Magnetic fields from $B=0$ to 6 T were applied parallel to the excitation and collection axis (the Faraday geometry). We used linearly polarized light from a continuous wave (CW) 532 nm doubled Nd:YAG laser to create electron-hole pairs far from the band edge and avoid optical pumping. The circular polarization of the PL light was analyzed by combining a linear polarizer with a 20 kHz photoelastic modulator set as a $\pm\lambda/4$ retarder at 1.55 μm.

We analyze our results by focusing on the degree of circular polarization, $\rho^*=(I_{\sigma^+}-I_{\sigma^-})/(I_{\sigma^+}+I_{\sigma^-})$, where $I_{\sigma^+}(I_{\sigma^-})$ is the intensity of the right (left) circularly polarized light. Figure 2(a) shows the dependence of ρ^* on magnetic field for sample 2 at 5.6 K. The linear behavior indicates that the Zeeman splitting, $g\mu_B B$, is much smaller than $k_B T$, and much larger than the electron-hole exchange interaction.[27,28] Moreover, data taken at very low magnetic fields [Fig. 2(a), inset] show no discontinuity around zero field, consistent with a very small exchange interaction.

In a simple two-level model the polarization would be described by the Brillouin function[29]

$$\rho^* = \tanh[g\mu_B B/2k_B T]. \quad (1)$$

For small values of $g\mu_B B/2k_B T$, Eq. (1) indeed predicts ρ^* to be linear in the field B, and thus a two-level model appears to describe satisfactorily the data in Fig. 2(a). But Eq. (1) also predicts that, at high temperature, ρ^* is linear in the inverse temperature, $1/T$. The temperature-dependent data in Fig. 2(b) show that this prediction is only borne out at very high temperatures. A more systematic test of Eq. (1) is made in Fig. 2(c), where the data from both Figs. 2(a) and 2(b) are plotted with respect to $\mu_B B/k_B T$. The thin dotted curve shows the best fit of Eq. (1) to these data. The fit is unsatisfactory and thus establishes that a two-level model is not adequate after all.

The need for a different model is also evident from our ODMR results. This technique monitors the difference of the

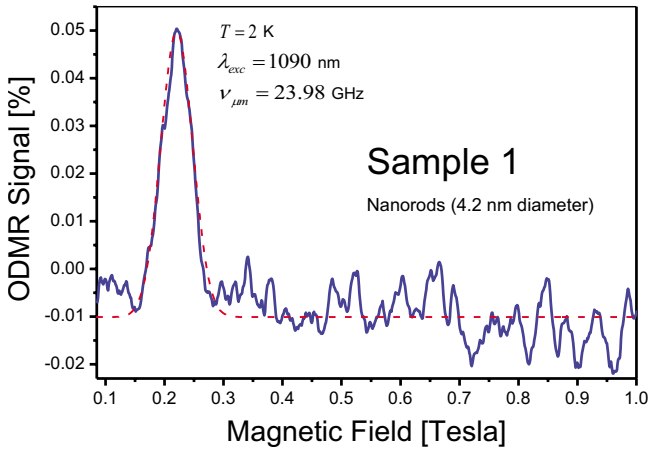

FIG. 3. (Color online) ODMR signal for NRs at 1.6 K.

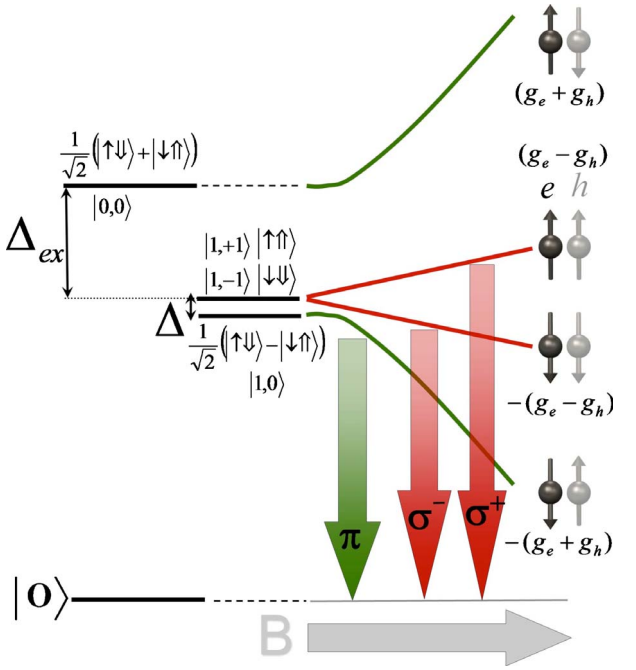

FIG. 4. (Color online) Schematic of the excitonic fine structure of PbSe nanostructures and its dependence on a magnetic field, B, in the case $g_e > g_h > 0$. Green arrow shows optical transition emitting linearly polarized light. Brown arrows show optical transitions emitting circularly polarized light.

total PL intensity with and without microwave excitation, as a function of the magnetic field.[21] When the energy of the microwave photons (0.1 meV in our case) equals the Zeeman splitting of two exciton levels for a particular magnetic-field strength, a spin-flip transition occurs between the levels. Because the recombination times of the exciton levels are different, this transition alters the intensity of the PL. The ODMR data in Fig. 3 reveal a single resonance at 0.22 T for sample 2 (mixed NRs and NCs) and no resonance for sample 1 (only NCs). In a two-level model the resonance at 0.22 T would correspond to an unrealistically large g factor (>7) and nearly 100% polarization even at the low fields and high temperatures studied, in contradiction with the data of Fig. 2.

We now show that our data can be understood within a standard singlet-triplet model, illustrated in Fig. 4, in which the exciton ground state has a fourfold degeneracy split by electron-hole exchange interactions and by shape anisotropy. This model is appropriate because in PbSe, at the L point, electrons and holes both have spin 1/2.[30,31] In spherical NCs the electron-hole exchange interaction splits the fourfold degenerate exciton state into a singlet state ($J=0$) and a threefold degenerate triplet state ($J=1$).[32] The wave function of the singlet state is $|J,m_J\rangle=|0,0\rangle=(|\uparrow\Downarrow\rangle+|\downarrow\Uparrow\rangle)/\sqrt{2}$, where ($\uparrow/\downarrow$) and ($\Uparrow/\Downarrow$) denote the spin projections of the electron and hole, respectively. The wave functions of the triplet states are $|1,0\rangle=(|\uparrow\Downarrow\rangle-|\downarrow\Uparrow\rangle)/\sqrt{2}$, $|1,+1\rangle=|\uparrow\Uparrow\rangle$, and $|1,-1\rangle=|\downarrow\Downarrow\rangle$. In the spherical approximation, the energy difference between the singlet and the threefold degenerate triplet states would be given by the electron-hole exchange energy, Δ_0. Shape anisotropy splits the $|1,0\rangle$ and $|1,\pm1\rangle$ states by Δ and increases the energy difference between the $|0,0\rangle$ and $|1,\pm1\rangle$ states to Δ_{ex}.[20,26] We note that this model assumes that both Δ_{ex} and Δ are much smaller than the intervalley splitting of the electron and hole states. This assumption is consistent with recent first-principles calculations.[16]

In the presence of an external magnetic field these four exciton levels will be split by the Zeeman terms $H_{\text{electron}} \equiv (g_e\mu_B\vec{B}\cdot\vec{s}_e)$ and $H_{\text{hole}} \equiv -(g_h\mu_B\vec{B}\cdot\vec{s}_h)$, where g_e and g_h are the g factors of the electron and hole, and s_e and s_h are their spin projections ($\pm1/2$). Figure 4 illustrates a key feature of this splitting: the two states with $m_j=0$ shift much faster with field than do the two states with $m_j=\pm1$. This is because the effective g factors of the $|0,0\rangle$ and $|1,0\rangle$ states are given by the sums $\pm(g_e+g_h)$, respectively, while for the $|1,\pm1\rangle$ states the effective g factors are given by the differences $\pm(g_e-g_h)$. Three features of the data in Fig. 2 lead to the conclusion that g_e+g_h is much larger than g_e-g_h. (1) The absence of any level crossings (which would lead to nonmonotonic polarization) implies that g_e+g_h is larger than g_e-g_h. (2) The sign of the polarization is always negative, which implies $g_e>g_h$. Therefore both g_e and g_h must be positive. (3) The small polarization (less than 10%) even in large fields (6 T) and at low temperature (5.6 K) imply that g_e-g_h is small, and hence that g_e and g_h are comparable. Together, these features imply that g_e+g_h is much larger than g_e-g_h and hence that the splitting rate of the $|0,0\rangle$ and $|1,0\rangle$ states is much larger than that of the $|1,\pm1\rangle$ states.

Although our model has four exciton levels, at low temperatures we only need to consider luminescence from the lower three levels. This is because the exchange energy Δ_{ex} is several tens of meV,[15,33,34] rendering the $|0,0\rangle$ state thermally inaccessible at our experimental temperatures. Of the three remaining levels, luminescence from the $|1,0\rangle$ state must be linearly polarized, and hence all circularly polarized light must originate from the triplet states $|1,1\rangle$ and $|1,-1\rangle$. Triplet states are often optically passive (because of angular momentum selection rules) and it is not clear what mechanism activates them here.

By considering the thermal population of the three lower levels, we then obtain an expression for the polarization different from that of Eq. (1):

$$\rho^* = \frac{3}{4}\tanh\left[\frac{1}{2}\frac{(g_e - g_h)\mu_B B}{k_B T}\right]\frac{\cosh\left[\frac{1}{2}\frac{(g_e - g_h)\mu_B B}{k_B T}\right]}{\cosh\left[\frac{1}{2}\frac{(g_e - g_h)\mu_B B}{k_B T}\right] + \frac{\tau_1^T}{2\tau_0^T}e^{(\Delta/k_B T)}e^{[1/2[(g_e+g_h)\mu_B B]/k_B T]}}, \quad (2)$$

where τ_0^T and τ_1^T are the exciton lifetimes from the $|1,0\rangle$ and $|1,\pm 1\rangle$ states, respectively. If τ_0^T is comparable or shorter than τ_1^T then Eq. (2) predicts a suppressed polarization [compared to Eq. (1)] at low temperatures, consistent with the data in Fig. 2(b). Physically, this suppression originates from the rapid depopulation of the $|1,\pm 1\rangle$ states at low temperatures (or in large fields), which in turn arises from the fast downward splitting of the $|0,0\rangle$ state.

The absence of discontinuities and linear dependence of the degree of polarization at low magnetic fields [Fig. 2(a), inset] indicates that Δ is much smaller than ~ 500 μeV, the thermal energy at 5.6 K. This assumption is confirmed by replotting the NR data in Figs. 2(a) and 2(b) as a function of $(\mu_B B/k_B T)$. Figures 2(c) shows that the data collapse onto a single curve; the same is true for NC data [Fig. 2(d)]. This means that the term $e^{(\Delta/k_B T)}$ in Eq. (2) is close to unity and therefore that Δ is much less that kT.

To obtain numerical values for g_e and g_h, we performed a least-squares fit of the expression in Eq. (2) to the data in Figs. 2(c) and 2(d). We took Δ to be zero, which simplifies the analysis but does not affect the results, and we constrained the g factors for the NRs and NCs to be equal. This constraint is reasonable because g factors are roughly proportional to band gaps, and the band gaps of our NRs and NCs are very similar. We allowed the ratio $\tau_1^T/2\tau_0^T$ to be different for NRs and NCs. This is because the small oscillator transition strength of the optically dark $|1,0\rangle$ state in spherically symmetric NCs is increased dramatically in NRs by the absence of the dielectric screening of the electric-field component parallel to the NR axis. This enhances the interaction of light with the $|1,0\rangle$ state, which also has a dipole moment along the rod axis. The fits are shown in Figs. 2(c) and 2(d) as heavy gray curves and provide an excellent description of the data, unlike the simple two-level model (shown as a thin dotted curve). The fitted parameter values are $g_e = +1.2 \pm 0.1$ and $g_h = +0.8 \pm 0.1$, with $\tau_1^T/2\tau_0^T = 0.44 \pm 0.04$ for NRs and $\tau_1^T/2\tau_0^T = 0.005 \pm 0.03$ for NCs.

Now we use our model to interpret our ODMR data. The relevant spin-flip transitions are from the $|1,0\rangle$ state into the $|1,+1\rangle$ and $|1,-1\rangle$ states. A resonance will thus occur under either of the conditions

$$h\nu = g_e \mu_B B + \Delta, \quad (3)$$

$$h\nu = g_h \mu_B B + \Delta. \quad (4)$$

These conditions are independent. In principle, we therefore expect resonances at two different values of the magnetic field: a lower field B_e (for transitions from $|1,0\rangle$ into $|1,+1\rangle$) and an upper field B_h (for transitions from $|1,0\rangle$ into $|1,-1\rangle$). In practice, these fields are not sufficiently well separated to be resolved. Consequently we assume that the ODMR signal (for the NR sample), which is centered at $B = 0.22$ T, is the superposition of two resonances at B_e and B_h. Using the g factors obtained above, we solve Eqs. (3) and (4) to obtain $\Delta = 88$ μeV. The resonance fields (for photon energy $h\nu = 100$ μeV) are $B_e = 0.18$ T and $B_{h=}0.26$ T. These fall within the width of the broad ODMR signal and hence justify our superposition assumption. The fact that the ODMR signal for NRs is positive corroborates that $\tau_1^T/2\tau_0^T < 1$.

We did not find any ODMR resonances from spherical NCs. This suggests that Δ is significantly smaller than in NRs. As a result, the energy of the spin-flip transitions is less than 0.1 meV and is thus undetectable in our experiment. For the electron g factor of 1.2, the upper bound for Δ in spherical NCs is 20 μeV.

The data reported here and the model proposed are qualitatively consistent with previous experimental work on the fine structure of PbSe NCs.[15,17,35,36] Several of these works reported time-resolved PL measurements on spherical NCs. Figure 5 shows the reported temperature dependence of PL lifetimes for NCs with diameter 4.6 nm (the same size as in our sample 2), as reported in Ref. 15, as well as for NCs with diameter close to 3.7 nm, as reported in Refs. 15 and 17. The lifetimes in all samples decrease with temperature and exhibit two plateaus. These plateaus strongly suggest that transitions between three distinct levels contribute to the PL,

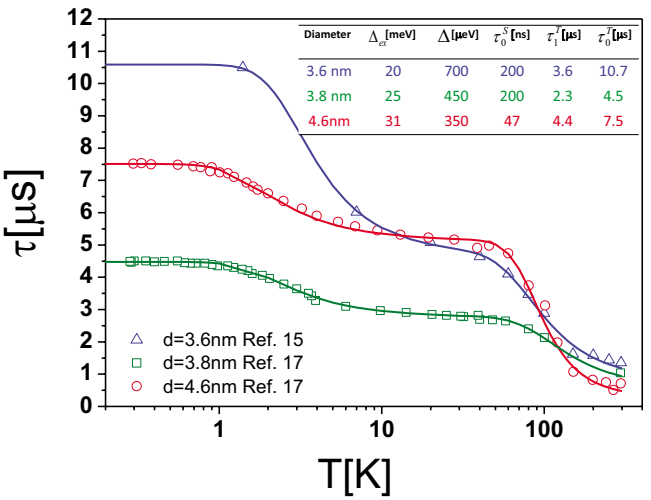

FIG. 5. (Color online) Photoluminescence lifetime of PbSe NCs reproduced from Refs. 15 and 17, as a function of temperature, for several NC diameters. Solid lines and tabulated parameter values are from fits to Eq. (5).

with the highest-lying level having the shortest lifetime (of order tens of nanoseconds) and the lowest-lying level having the longest lifetime (of order several microseconds).

In our model there are three levels in zero magnetic field. The highest-lying level is the $|0,0\rangle$ singlet state, the lowest-lying is the $|1,0\rangle$ triplet state, and the intermediate level is the twofold-degenerate $|1,\pm 1\rangle$ state of the triplet. By assuming that the populations of these levels are in thermal equilibrium we find that the temperature dependence of the radiative lifetime in the absence of nonradiative mechanisms is given by

$$\tau(T) = \frac{(1 + 2e^{-\Delta/k_BT} + e^{-(\Delta+\Delta_{ex})/k_BT})}{\left(\frac{1}{\tau_0^T} + \frac{2e^{-\Delta/k_BT}}{\tau_1^T} + \frac{e^{-(\Delta+\Delta_{ex})/k_BT}}{\tau_0^S}\right)}, \quad (5)$$

where τ_0^S is the radiative lifetime of the $|0,0\rangle$ singlet state. By fitting this expression to three sets of published data we extracted values for Δ_{ex}, Δ, τ_0^S, τ_0^T, and τ_1^T. These values, which are listed in Fig. 5, are in qualitative agreement with our findings. Broadly speaking, the lifetime data suggests a high-lying short-lived state (a bright singlet in our model) separated by several tens of meV (Δ_{ex}) from a lower-lying long-lived state (a triplet), which in turn is split by a few hundred μeV(Δ). Furthermore, the lifetime of the lower energy triplet state, τ_0^T, is longer than those of the upper ones, τ_1^T. The lifetime measurements give values for Δ_{ex} smaller than do other experiments[33,37] and theory,[16] and values for $\tau_1^T/2\tau_0^T$ and Δ larger than do our CP-MPL and ODMR results. We hypothesize that these discrepancies may originate from the influence of ligands and environment, which can alter lifetimes by creating nonradiative decay channels.[15,35,36] This suggestion is supported by reports, from Refs. 15 and 17, of different lifetimes for NCs of the same size ($\sim$3.7 nm), as shown in Fig. 5.

The applicability of the singlet triplet-model for describing the fine structure of the band-edge excitons in spherical PbSe NCs and NRs requires a large intervalley splitting of the band-edge electron and holes states. In this case the Bloch wave functions of the ground electron and hole states are the symmetric (a_1) linear combinations of the four identical valleys. This approximation is valid if the intervalley splitting is significantly larger than both the electron-hole exchange interaction and the splittings that arise from asymmetry of the NCs.

In summary, we used circularly polarized magnetophotoluminescence and optically detected magnetic resonance spectroscopies to study the fine structure of band-edge excitons in PbSe NCs and [001]-oriented NRs. We find that the ground exciton state is well described by a singlet-triplet model consisting of an upper bright singlet state not populated at low temperature, and an unusual optically active triplet state. Analyses of the magneto-optical data gives g factors of electrons and holes as $g_e = +1.2 \pm 0.1$ and $g_h = +0.8 \pm 0.1$, respectively.

J.E.B acknowledges the National Research Council postdoctoral program, while the Office of Naval Research (ONR) is gratefully acknowledged for financial support of this work.

[1] A. Fu, W. Gu, B. Boussert, K. Koski, D. Gerion, L. Manna, M. Le Gros, C. A. Larabell, and A. P. Alivisatos, Nano Lett. **7**, 179 (2007).
[2] B. Dubertret, P. Skourides, D. J. Norris, V. Noireaux, A. H. Brivanlou, and A. Libchaber, Science **298**, 1759 (2002).
[3] J. M. Pietryga, D. J. Werder, D. J. Williams, J. L. Casson, R. D. Schaller, V. I. Klimov, and J. A. Hollingsworth, J. Am. Chem. Soc. **130**, 4879 (2008).
[4] J. M. Caruge, J. E. Halpert, V. Wood, V. Bulovic, and M. G. Bawendi, Nat. Photonics **2**, 247 (2008).
[5] V. I. Klimov, A. A. Mikhailovsky, S. Xu, A. V. Malko, J. A. Hollingsworth, C. A. Leatherdale, H.-J. Eisler, and M. G. Bawendi, Science **290**, 314 (2000).
[6] V. Sukhovatkin, S. Hinds, L. Brzozowski, and E. H. Sargent, Science **324**, 1542 (2009).
[7] E. H. Sargent, Nat. Photonics **3**, 325 (2009).
[8] R. D. Schaller, M. Sykora, J. M. Pietryga, and V. I. Klimov, Nano Lett. **6**, 424 (2006).
[9] A. J. Nozik, Chem. Phys. Lett. **457**, 3 (2008).
[10] W. Ma, J. M. Luther, H. Zheng, Y. Wu, and A. P. Alivisatos, Nano Lett. **9**, 1699 (2009).
[11] J. J. Choi, Y. F. Lim, M. B. Santiago-Berrios, M. Oh, B. R. Hyun, L. Sun, A. C. Bartnik, A. Goedhart, G. G. Malliaras, H. D. Abruña, F. W. Wise, and T. Hanrath, Nano Lett. **9**, 3749 (2009).
[12] R. D. Schaller, M. A. Petruska, and V. I. Klimov, J. Phys. Chem. B **107**, 13765 (2003).
[13] B. R. Hyun, H. Chen, D. A. Rey, F. W. Wise, and C. A. Batt, J. Phys. Chem. B **111**, 5726 (2007).
[14] I. Kang and F. W. Wise, J. Opt. Soc. Am. B **14**, 1632 (1997).
[15] A. Kigel, M. Brumer, G. I. Maikov, A. Sashchiuk, and E. Lifshitz, Small **5**, 1675 (2009).
[16] J. M. An, A. Franceschetti, and A. Zunger, Nano Lett. **7**, 2129 (2007).
[17] R. D. Schaller, S. A. Crooker, D. A. Bussian, J. M. Pietryga, J. Joo, and V. I. Klimov, Phys. Rev. Lett. **105**, 067403 (2010).
[18] M. Nirmal, D. J. Norris, M. Kuno, M. G. Bawendi, Al. L. Efros, and M. Rosen, Phys. Rev. Lett. **75**, 3728 (1995).
[19] D. J. Norris, Al. L. Efros, M. Rosen, and M. G. Bawendi, Phys. Rev. B **53**, 16347 (1996).
[20] Al. L. Efros, M. Rosen, M. Kuno, M. Nirmal, D. J. Norris, and M. G. Bawendi, Phys. Rev. B **54**, 4843 (1996).
[21] T. A. Kennedy and E. R. Glaser, *Identification of Defects in Semiconductors, Semiconductors and Semimetals* (Academic Press, New York, 1998), Vol. 51A, Chaps. 3 and 93.
[22] E. Lifshitz, L. Fradkin, A. Glozman, and L. Langof, Annu. Rev. Phys. Chem. **55**, 509 (2004).
[23] W. W. Yu, J. C. Falkner, B. S. Shin, and V. L. Colvin, Chem. Mater. **16**, 3318 (2004).
[24] R. J. Ellingson, M. C. Beard, J. C. Johnson, P. Yu, O. I. Micic,

A. J. Nozik, A. Shabaev, and Al. L Efros, Nano Lett. **5**, 865 (2005).
[25] W. K. Koh, A. C. Bartnik, F. W. Wise, and C. B. Murray, J. Am. Chem. Soc. **132**, 3909 (2010).
[26] A. Shabaev, and Al. L Efros, Nano Lett. **4**, 1821 (2004).
[27] V. D. Kulakovskii, G. Bacher, R. Weigand, T. Kummell, A. Forchel, E. Borovitskaya, K. Leonardi, and D. Hommel, Phys. Rev. Lett. **82**, 1780 (1999).
[28] D. Gammon, Al. L. Efros, T. A. Kennedy, M. Rosen, D. S. Katzer, D. Park, S. W. Brown, V. L. Korenev, and I. A. Merkulov, Phys. Rev. Lett. **86**, 5176 (2001).
[29] C. Kittel, *Introduction to Solid State Physics*, 6th ed. (Wiley and Sons, New York, 1986), Vol. 402, Chap. 14.
[30] D. L. Mitchel, E. D. Palick, and J. N. Zemel, in *Proceeding of the International Conference on the Physics of Semiconductors*, Paris, 1964 (Academic Press Inc., New York, 1965), p. 325.
[31] D. L. Mitchell and R. F. Wallis, Phys. Rev. **151**, 581 (1966).
[32] E. Johnston-Halperin, D. D. Awschalom, S. A. Crooker, Al. L. Efros, M. Rosen, X. Peng, and A. P. Alivisatos, Phys. Rev. B **63**, 205309 (2001).
[33] J. G. Tischler *et al.* (unpublished).
[34] R. Espiau de Lamaëstre, H. Bernas, D. Pacifici, G. Franzó, and F. Priolo, Appl. Phys. Lett. **88**, 181115 (2006).
[35] H. Liu and P. Guyot-Sionnest, J. Phys. Chem. C **114**, 14860 (2010).
[36] O. E. Semonin, J. C. Johnson, J. M. Luther, A. G. Midgett, A. J. Nozik, and M. C. J. Beard, Phys. Chem. Lett. **1**, 2445 (2010).
[37] E. Lifshitz, M. Brumer, A. Kigel, A. Sashchiuk, M. Bashouti, M. Sirota, E. Galun, Z. Burshtein, A. Q. Le Quang, I. Ledoux-Rak, and J. Zyss, J. Phys. Chem. B **110**, 25356 (2006).